Biomed Microdevices (2016) 18: 68
DOI 10.1007/s10544-016-0099-2

Numerical and experimental study of capillary-driven flow of PCR solution in hybrid hydrophobic microfluidic networks

Naveen Ramalingam[1,2] · **Majid Ebrahimi Warkiani**[3] · **Neevan Ramalingam**[4] · **Gholamreza Keshavarzi**[3] · **Liu Hao-Bing**[2,5] · **Thomas Gong Hai-Qing**[2]

Published online: 18 July 2016

Abstract Capillary-driven microfluidics is essential for development of point-of-care diagnostic micro-devices. Polymerase chain reaction (PCR)-based micro-devices are widely developed and used in such point-of-care settings. It is imperative to characterize the fluid parameters of PCR solution for designing efficient capillary-driven microfluidic networks. Generally, for numeric modelling, the fluid parameters of PCR solution are approximated to that of water. This procedure leads to inaccurate results, which are discrepant to experimental data. This paper describes mathematical modeling and experimental validation of capillary-driven flow inside Poly-(dimethyl) siloxane (PDMS)-glass hybrid microchannels. Using experimentally measured PCR fluid parameters, the capillary meniscus displacement in PDMS-glass microfluidic ladder network is simulated using computational fluid dynamic (CFD), and experimentally verified to match with the simulated data.

Keywords Microfluidics · Capillary · Polymerase chain reaction (PCR) · Surface hydrophobicity · Simulation

1 Introduction

Polymerase chain reaction (PCR) is enzyme-based process that is widely used for genomic and transcriptomic applications. Numerous groups have successfully implemented PCR in microfluidics devices (Zhang and Xing 2007). Liquid flow in such microdevices are either achieved by active or passive pumps (Au et al. 2011). Active pumping methods require sophisticated peripheral and bulky instruments and also have substantial dead volumes. However, for point-of-care applications it is desired to propel liquids (test sample, sample preparation buffers, PCR solution, etc.) using passive microfluidics, which do not require external pressure source or peripheral instruments. Passive capillary driven microfluidics can be broadly classified into two categories: I) Methods which use porous capillary membrane (also known as fibrous microfluidics), and II) Methods which do not use membranes. Fibrous microfluidics majorly use nitrocellulose, thread, yarns, silk, and paper as a substrate. Although there is a huge interest in fibrous microfluidics (Hu et al. 2014) for its simplicity, point-of-care use and most importantly economical for use in under-developed countries, these devices in the current format suffer from limited multiplexing capability and limit of detection when compared to classical ELISA methods (Safavieh and Juncker 2013).

This research was performed while Naveen Ramalingam and Liu Hao-Bing were at School of Mechanical and Aerospace Engineering, Nanyang Technological University, 639798, Singapore.

Electronic supplementary material The online version of this article (doi:10.1007/s10544-016-0099-2) contains supplementary material, which is available to authorized users.

✉ Naveen Ramalingam
naveensma@gmail.com

✉ Thomas Gong Hai-Qing
mhqgong@ntu.edu.sg

[1] Fluidigm Corporation, 7000 Shoreline Court, South San Francisco, CA 94080, USA

[2] School of Mechanical and Aerospace Engineering, Nanyang Technological University, Singapore 639798, Singapore

[3] School of Mechanical and Manufacturing Engineering, Australian Center for NanoMedicine, University of New South Wales, Sydney 2052, Australia

[4] Department of Electrical and Computer Engineering, Iowa State University, Ames, IA 50011, USA

[5] Wisewater Pte Ltd., 71 Ayer Rajah Crescent, Singapore 139951, Singapore

Other capillary driven microfluidics, which do not use membranes include capillary pump (Zimmermann et al. 2007), Poly-(dimethyl) siloxane (PDMS) permeation-driven (Randall and Doyle 2005), and vacuum-driven methods (Hosokawa et al. 2006). Walker et al. reported a hybrid strategy to combine active and passive microfluidics (Walker and Beebe 2002). In this work, capillary microfluidics is activated by positive pressure imposed by the hemispheric droplet dispensed on top of the inlet. It is a challenge to activate capillary microfluidics with purely passive capillary components. Activation of capillary microfluidics in devices depends on many factors such as fluid parameters, chemistry, substrate type (hydrophilic or hydrophobic) and geometry of the microstructures. The performance requirement of a particular application generally imposes constrain on the fluid parameters. Hence, choice of substrate type, selection of chemistry on the surface and microfluidic network design are crucial for capillary microfluidics.

In the past, capillary-driven microfluidics has been successfully implemented for one-step immunoassays, plasma extraction, and continuous-flow PCR in various device formats and substrates (Delamarche et al. 1997; Gervais and Delamarche 2009, Juncker et al. 2002; Kim et al. 1995, 2010; Safavieh and Juncker 2013, Safavieh et al. 2014; Tachibana et al. 2015; Zimmermann et al. 2007). Whiteside's group at Harvard first introduced micromolding in capillaries (also known as MIMIC) to fabricate different polymer microstructures on a desired substrate (Kim et al. 1995). In this work, Kim et al. reported successful filling of the PDMS-glass microchannels using pre-polymer fluid with low surface-tension. Subsequently this idea was further developed in the last decade by Delamarche group at IBM Zurich for various immunoassay applications. Since the surface tension of the fluid interacts with the surface of channels, it is essential to understand the surface type and chemistry of the substrate material, which harbors the channels (contributes to three sides of the microchannel). In literature, different research groups have used different hybrid microstructures such as PDMS(substrate that harbors channel)-glass/silicon (Kim et al. 1995, 2010; Ramalingam et al. 2009), Silicon(channel)-PDMS (Juncker et al. 2002), PDMS(channel)-Silicon (Gervais and Delamarche 2009, Zimmermann et al. 2007), and Silicon(channel)-glass (Tachibana et al. 2015). Unmodified silicon and glass are hydrophilic, and PDMS is hydrophobic. For ease in fabrication, microfluidic channels are widely fabricated using PDMS and attached to a support like glass or silicon. Hence, it is a challenge to activate capillary filling of liquids with high surface tension (contact angle $\geq 90°$) in devices, where channels are fabricated on PDMS and attached to either glass or silicon. Capillary in such micro devices can be activated either by modifying the PDMS surface to increase its interfacial free energy or reducing the surface tension of the fluid. The surface of the PDMS can be modified by plasma treatment (Kim et al. 1995), adsorbing bovine serum albumin (BSA) (Kim et al. 1995) or chemically doping the PDMS with surfactant such as Triton X-100 (Seo and Lee 2006) or Silwet L-77 (Kim et al. 2010). Delamarche and colleagues employed plasma treatment to render the PDMS surface hydrophilic in order to fill the channels with immunoglobulins (Delamarche et al. 1997). However, the PDMS can recover its hydrophobic characteristics in few hours thereby limiting long-term usage of treated channels. Capillary microfluidics has been demonstrated in PDMS and silicon hybrid microchannels. The capillary microfluidic was achieved by either treating the silicon surface with thiolated polyethylene glycol (PEG) (Juncker et al. 2002) or with Pluronic (Gervais and Delamarche 2009). Such methods requires extra chip fabrication step. A simple strategy to activate capillary microfluidics in PDMS-glass microchannel is to add organic solvent or surfactant to the test fluid (Ramalingam et al. 2009). In Kim et al., the authors added ethanol (organic solvent) to lower the surface tension of water and activate capillary. It should be noted that the biological application type may impose constrain on the addition of organic solvent to the test fluid. We have previously developed and validated a range of capillary-driven microfluidic biochips for various point-of-care, PCR-based diagnostic applications (Ramalingam et al. 2009, 2010). In our previous work, we reported a simple PCR-compatible method to activate capillary-driven flow in hydrophobic PDMS(channel)-glass by implementing a soluble surfactant (Ramalingam et al. 2009). The compatibility of the non-ionic surfactant with PCR, and its effect on PCR solution parameters is extensively studied and reported in this work.

In order to design efficient capillary-driven microfluidic networks using computational fluid dynamic software's (e.g., COMSOL or ANSYS Fluent), it is imperative to characterise the fluid parameters of PCR solution for achieving accurate results, which match with the experimental data. Unfortunately, most studies involving numerical simulation of thermal and kinematic properties of PCR solution in microfluidic devices often approximate the flow properties of PCR solution to that of pure water (Chen et al. 2012; Gui and Ren 2006, Siegrist et al. 2010; Wang and Wang 2010). However, based on our experimental results, the kinetic properties of PCR solution is different from that of pure water. Simulation of PCR-based micro devices with water parameters will lead to contradicting results, which do not match with the experimental data. To complicate further, components and concentration of PCR master-mix vary significantly among different vendors, and these variations, change the fluid parameters significantly. Hence, it is necessary to characterize the kinetic property of each PCR solution for efficient math-aided design of PCR-based microfluidic devices. In this work, we have characterized the kinetic properties such as surface tension and contact angle of the PCR solution. Using these parameters, the capillary filling fluid front was simulated

using volume of fluid (VOF) model, and experimentally validated. The work reported in this article is an extension of our previous work. For further information on the development and characterization of the capillary ladder network chip, the readers are directed to the publication by Ramalingam et al. (Ramalingam et al. 2009).

2 Materials and methods

2.1 Chip design

In this study, the capillary-driven flow of PCR solution in a 24 mm long and 2.5 mm wide rectangular inlet channel is studied. The dimension of different structures on the microfluidic device is shown in Fig. 1. The depth of the entire microchannel on the device is ~90 μm. The mouth of the inlet channel is 1 mm wide with an expansion angle of 26°. The inlet channel feeds twelve micro-reactors, which are orthogonally oriented to the inlet channel. A micro-reactor is composed of a 1.5 mm long inlet bridge channel connected to a central reactor of 4 mm long × 1 mm wide through an expansion angle of 16°. During microfluidic loading of PCR solution, the air inside the micro-reactors is purged to a common outlet channel connected through an outlet bridge channel. The dimensions of outlet bridge channel and air-venting channel are same as the inlet bridge channel and inlet channel respectively.

2.2 Composition of different PCR solutions

The polymerase chain reaction solution (10 μl) contains 20 mM Tris-HCl (pH 8.4), 50 mM KCl (Invitrogen buffer by Life Technologies, Carlsbad, P/N 10966), 0.2 mM each of dATP, dCTP, dTTP and dGTP (PCR Nucleotide Mix, Promega, Madison, P/N C1141), 3 mM $MgCl_2$ (Invitrogen by Life Technologies, Carlsbad, P/N 10966), 0.3 μM each of forward and reverse gene specific primer (1st BASE, Singapore), 0.1 U/μl of hot-start Platinum *Taq* DNA polymerase (Invitrogen by Life Technologies, Carlsbad, P/N 10966), 1 μg/μl of non-acetylated bovine serum albumin (BSA) (Sigma Aldrich, St Louis, P/N B 8667), 1X SYBR Green I (Cambrex Biosciences, Maine, USA), and 0.1 ng/μl (3×10^7 copies) of plasmid pGEM-3Z DNA template. The plasmid contains BNI-1 fragment of SARS cDNA. The forward and reverse primer (forward primer sequence: 5'-ATG AAT TAC CAA GTC AAT GGT TAC-3' and reverse primer sequence: 5'-CAT AAC CAG TCG GTA CAG CTA-3') amplifies a 189 bp gene fragment. Henceforth, the above solution is known as "Invitrogen PCR solution". This solution failed to load into the PDMS/glass array chip by capillary action due to hydrophobic nature of the PDMS-glass microchannel. Hence, non-ionic surfactants, Triton X-100 (T8787, Sigma Aldrich, USA) at different concentrations (0.05 %, 0.1 %, 0.15 %, and 0.2 %) were added to activate the PCR solution flow under capillary action. Experiments indicate that 0.1 % of Triton X-100 can activate capillary flow. Hereafter, the "Invitrogen PCR solution" with 0.1 % Triton X-100 will be known as "modified Invitrogen PCR solution". Some commercial PCR buffers (M1902 Promega, Madison; F-514S & AB0192 Finnzyme/Thermo Fisher Scientific, Waltham; M0321S, New England Biolabs, Ipswich) contain 0.1 % Triton X-100 to enhance *Taq* Polymerase activity. It is thought Triton X-100 suppresses the formation of secondary nucleic-acid structure and aids amplification of a particular target (Bachmann et al. 1990). In order to circumvent the requirement to add Triton X-100 externally to the Invitrogen PCR solution, commercial PCR buffer containing Triton X-100 from Promega (M1902; 10 mM Tris-HCl (pH 9.0), 50 mM KCl, and 0.1 % Triton X-100) was used to replace the Invitrogen buffer in

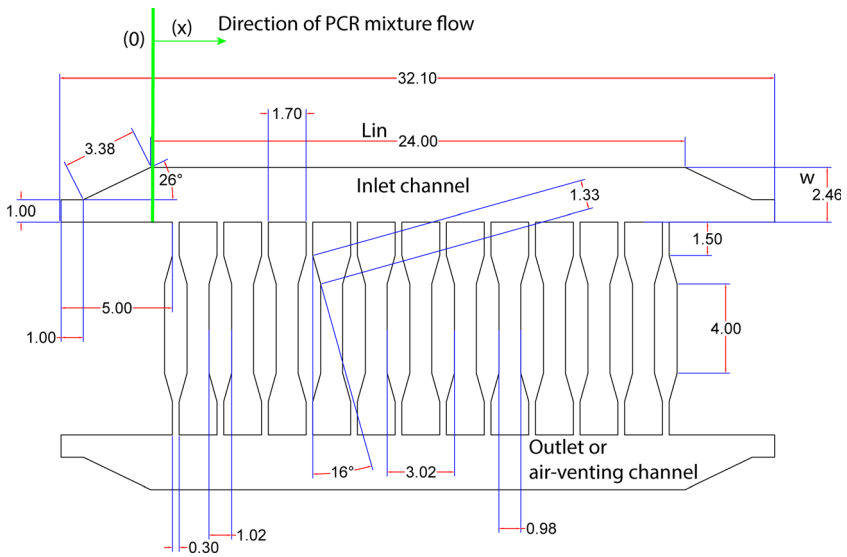

Fig. 1 Dimensioned inlet channel, micro reactor and outlet channel on a capillary microdevice used for mathematical modelling

Invitrogen PCR solution. The remaining components and concentrations were same as Invitrogen PCR solution. This solution with Promega buffer will be known as "Promega PCR solution". In order to understand the microfluidic characteristics of capillary-driven flow, contact angle and surface tension of different PCR solutions were experimentally determined.

3 Results and discussion

3.1 Effect of Triton X-100 concentration on contact angle of PCR solution

It is thought that higher concentration of Triton X-100 will lead to better wetting and increase the filling rate (Karagunduz et al. 2001). Hence, the effect of Triton X-100 concentration on contact angle of PCR solution on cured PDMS and acid-washed glass surface is studied. Invitrogen PCR solution (0 % TX-100) is spiked to get 4 different sets of PCR solution at 0.05 %, 0.1 %, 0.15 %, and 0.2 % Triton X-100 concentration (Fig. 2). For comparison, the contact angle of ultra-pure water (18.2 MΩ•cm resistivity at 25 °C; Simplicity 185 system from Millipore Corporation, Billerica, MA, USA) on cured PDMS and acid-washed glass substrate are measured. The contact angle of deionised water and Invitrogen PCR solution is comparable for both cured PDMS (~97°) and acid-washed glass substrate (~30°). However, with addition of 0.05 % Triton X-100 to Invitrogen PCR solution, the contact angle drastically reduced both on cured PDMS (from 97° to 45.5°), and acid-washed glass (from 30° to 15.3°). Further addition of Triton X-100 (0.1 %, 0.15 % and 0.2 %), did not drastically change the contact angle of Invitrogen PCR solution on cured PDMS. On the other hand, with increase in Triton X-100 concentration, the contact angle of Invitrogen PCR solution further reduced (Fig. 2). In the PCR array chip reported in this paper, PDMS pre-polymer is used a liquid sealant to seal and isolate micro reactor. PDMS pre-polymer is loaded in both inlet and air-venting channel. Hence, the contact angle of PDMS pre-polymer on cured PDMS, and acid-washed glass substrate is experimentally determined. The contact angle of PDMS pre-polymer on both cured PDMS and acid-washed glass substrate is found to be comparable (14.1° on acid-washed glass; 15.6° on cured PDMS).

3.2 Effect of surfactant (Triton X-100) on threshold cycle, PCR yield, PCR efficiency and amplicon melting temperature

In order to achieve capillary microfluidics, it is essential that the PCR buffer contain surfactant such as Triton X-100 or Tween 20. Commercial PCR buffers, which do not contain Triton X-100/surfactant is spiked with 0.1 % Triton X-100. Higher concentration of detergents is advantageous for our capillary-based microfluidics. However, studies show that Triton X-100 inhibits PCR at concentrations higher than 5 % (*v*/v) (Weyant et al. 1990). In order to understand the effect of 0.1 % Triton X-100 addition on threshold cycle, PCR yield, PCR efficiency and amplicon melting temperature, 189-bp amplicon were analysed on RotorGene 3000. All reaction was tested in triplicates. For this experiment Invitrogen PCR buffer (pH 8.4;20 mM Tris-HCl,50 mM KCl) was spiked with

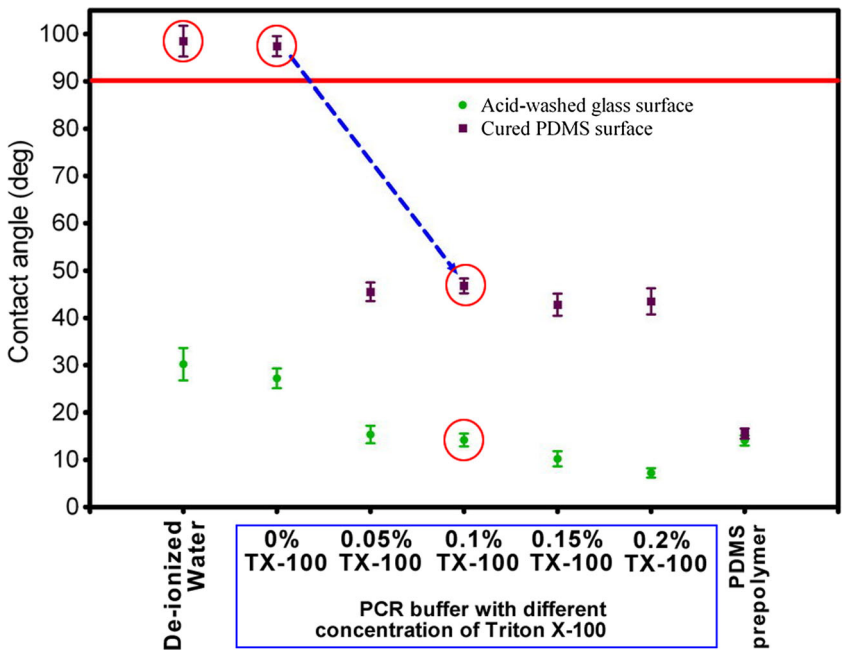

Fig. 2 Effect of Triton X-100 concentration on contact angle of PCR buffer on glass and PDMS surfaces. *Error bars* are standard deviation for $n = 5$ samples (n is number of technical replicates). PDMS pre-polymer is used as liquid sealant in the developed PCR chip

0.1 % Triton X-100 and tested. The control PCR buffer reaction contained Invitrogen buffer without Triton X-100 and a commercial buffer from Promega, which contains 0.1 % Triton X-100. It can be inferred from Fig. 3, that addition of 0.1 % did not affect the PCR performance metrics (Threshold cycle, PCR efficiency, melting temperature, and PCR yield). The use of Triton X-100 is advantageous for most of the primer-template systems including ours. However, it should be noted that this might not be a general case for other primer-template systems. It is advisable to optimize the concentration of Triton X-100 for each primer-template system.

3.3 Contact angle and surface tension measurement of PCR solution

The different types of PCR solution (test solutions):- Invitrogen PCR solution, Promega PCR solution, and PDMS pre-polymer used as liquid sealant were prepared freshly just before the measurements. The contact angle was measured by placing a 10 μl of sessile drop on the desired surface (cured PDMS/acid-washed glass) and using a FTA 200 (First Ten Angstroms, Virginia) instrument equipped with a monochrome 1/3″ medium resolution camera (KC-263C; Rapitron, Italy) at room temperature and ambient humidity.

The contact angle of Invitrogen PCR solution (lacks Triton X-100 surfactant) on cured PDMS, and acid-washed glass substrate are 97° and 30° respectively. Similarly, the contact angle of Promega PCR solution (contains 0.1 % Triton X-100 surfactant) on cured PDMS, and acid-washed glass substrate are 46° and 14° respectively (Fig. 4).

Surface tension values of the test solution were estimated through pendant drop shape analysis using a FTA 200 (First Ten Angstroms, Virginia) instrument. The surface tension measurement set-up is calibrated using ultra-pure water. The surface tension of ultra-pure water was estimated to be 71.48 ± 0.4 mN/m (n = 3), which is very close to the value (72 mN/m) from literature (Schutzius et al. 2012). The average surface tension of Invitrogen PCR solution and Promega PCR solution are found to be 69.75 mN/m and 30.8 mN/m (Fig. 5).

To test the reproducibility of PCR in micro reactors, a total of six micro reactors were loaded with 3×10^7 copies of SARS DNA template. The mean Ct value for amplification of 3×10^7 copies of SARS template DNA is 11.6 with a standard deviation of 0.12. The Ct values for amplification of 3×10^7 copies of template DNA in different micro reactors were consistent within a chip (Fig. 6).

3.4 Mathematical modelling of capillary meniscus movement

3.4.1 Theory

In the developed PCR array chip, the rectangular microchannel is composed of two substrates, glass substrum

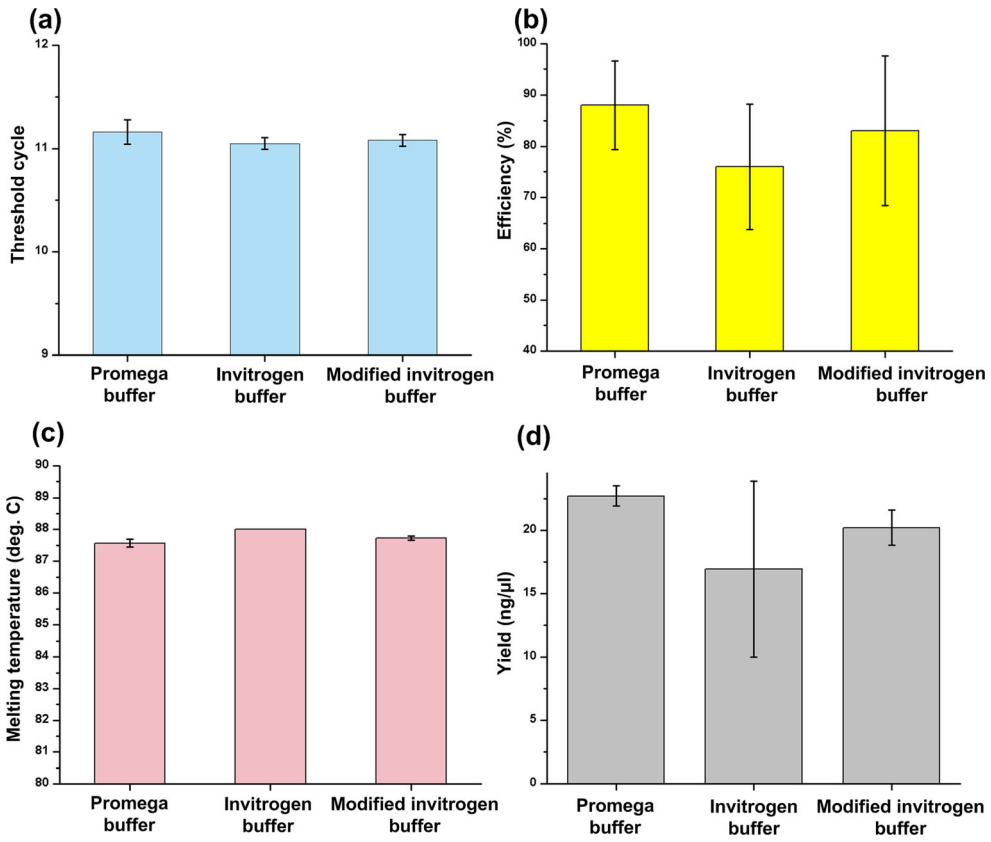

Fig. 3 Effect of Triton X-100 (0.1 %) on PCR performance metrics. **a** Threshold cycle of triplicate reactions. **b** PCR efficiency. **c** Melting temperature (Tm) of amplicon. **d** PCR yield quantified on Agilent Bioanalyzer. Composition of Promega buffer: (pH 9.0;10 mM Tris-HCl,50 mM KCl, 0.1 % Triton X-100). Composition of Invitrogen buffer: (pH 8.4;20 mM Tris-HCl,50 mM KCl). Composition of modified Invitrogen buffer: (pH 8.4;20 mM Tris-HCl,50 mM KCl,0.1 % Triton X-100). *Error bars* are SDs for triplicate reactions

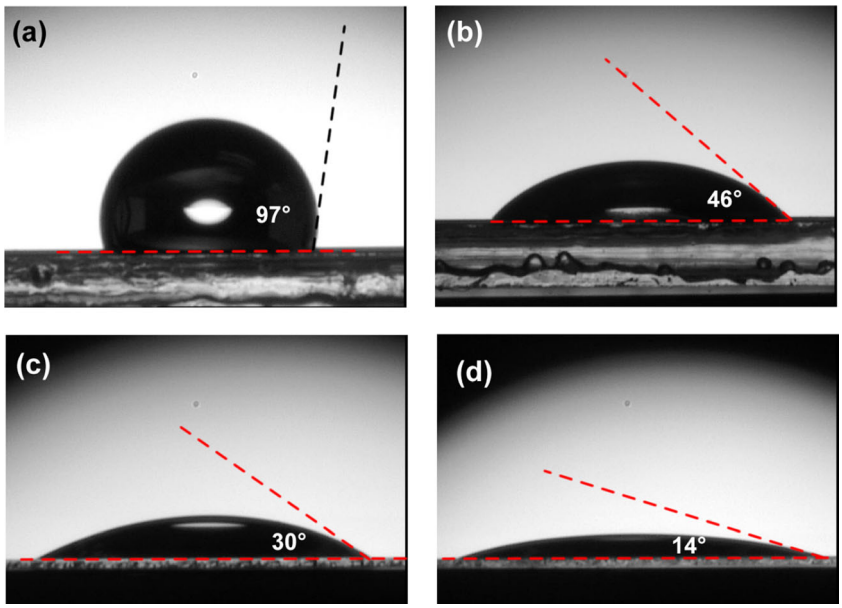

Fig. 4 Contact angle of PCR solution (Invitrogen and Promega) on cured PDMS layer and acid-washed glass substrate. **a** Contact angle of Invitrogen PCR solution (97°) on cured PDMS. **b** Contact angle of Promega PCR solution (46°) on cured PDMS. **c** Contact angle of Invitrogen PCR solution (30°) on acid-washed glass. **d** Contact of Promega PCR solution (14°) on acid-washed glass

(one face) and PDMS (three faces). If the surface tension of the fluid is below the surface energy of the solid, the liquid will spread on the surface. The contact angles of liquid/PCR solution on glass substrate and PDMS are denoted by θ_g

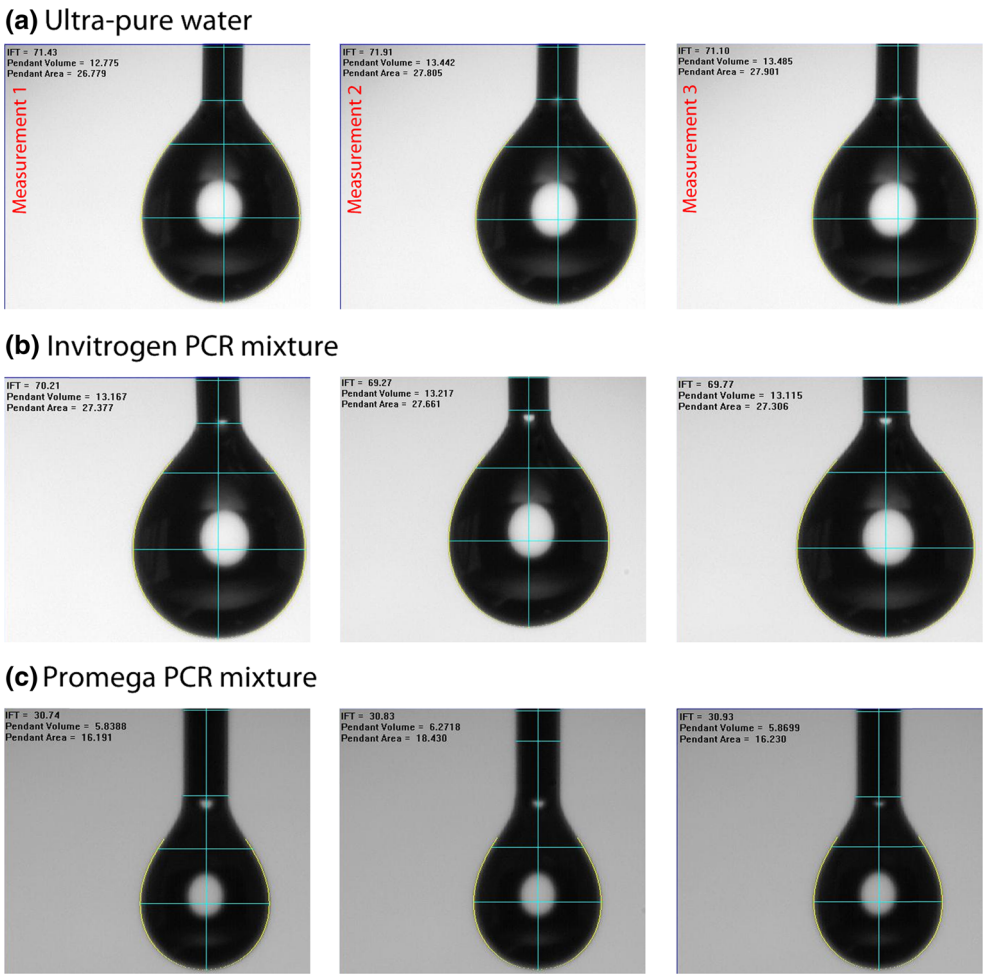

Fig. 5 Surface tension of test solution using drop shape method. **a** Ultra-pure water, **b** Invitrogen PCR solution and **c** Promega PCR solution

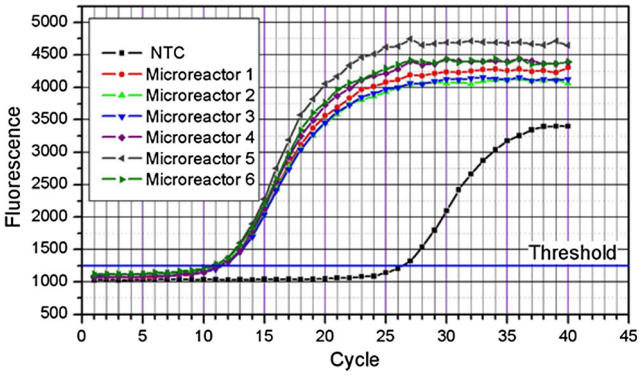

Fig. 6 Amplification plot to test the reproducibility of optimized PCR conditions in six micro reactors on a PDMS-glass chip

and θ_p respectively. The pressure drop at liquid-air interface inside a rectangular microchannel with two different surfaces is expressed by Young-Laplace equation (Yun and Yoon 2005).

$$p_C = \sigma_{PCR}\left(\frac{Cos\theta_g + Cos\theta_p}{d} + \frac{2Cos\theta_p}{w}\right) \tag{1}$$

Where P_c (P_c or $\Delta p = p_l - p_v$; p_l is pressure at liquid phase, p_v is pressure at vapour phase) is capillary pressure, σ_{PCR} is surface tension of PCR solution, d and w are depth and width of rectangular channel respectively, θ_p and θ_g are contact angle of PCR solution on PDMS, and acid-washed glass surface respectively. The equivalent force F experienced by the capillary fluid column along the x-direction is given by following equation.

$$F = P_C \times w \times d \tag{2}$$

When, $\Delta p = p_l - p_v > 0$ the channel is hydrophilic, and $\Delta p = p_l - p_v < 0$ the channel is hydrophobic. Where p_l and p_v are pressure at liquid and vapour/air.

3.4.2 Governing equations

The flow is considered laminar, incompressible, and Newtonian with isothermal condition. The governing equations are the Navier-Stokes and Continuity equation. The volumetric flowrate (dv/dt), in a rectangular channel for a Newtonian fluid is given by Eq. 3 (Jeong et al. 2007).

$$\frac{dV}{dt} = \frac{d(wdL(t))}{dt} = \frac{w \times d \times \Delta p \times c_g}{\eta L} \tag{3}$$

where w and d are width and depth of the inlet channel, $L(t)$ is the length of the horizontal capillary column from the origin of x-axis (refer to Fig. 1), η is the viscosity of PCR solution, Δp is the pressure drop across the distance L, and c_g is the shape factor given by an infinite series described by Eq. 4. (Bruus 2008)

$$c_{g=\frac{d^2}{12}}\left(1 - \sum_{i,odd}^{\infty} \frac{1}{i^5}\frac{192}{\pi^5}\frac{d}{w}\tanh\left[i\pi\frac{w}{2d}\right]\right) \tag{4}$$

The capillary pressure in the hybrid-PDMS glass microchannel is given in Eq. 1. By integration of Eq. 3, and use of approximation for the infinite series in Eq. 4.(Bruus 2008), the liquid meniscus position inside the rectangular microchannel is given by following Eq. 5.

$$L^2(t) = \left[\frac{d^2 \times \sigma_{PCR}}{6 \times \eta_{PCR}} \times \left(\frac{cos\theta_g + cos\theta_p}{d} + \frac{2cos\theta_p}{w}\right)\left(1 - 0.63\frac{d}{w}\right)\right] \times t \equiv a_t \times t \tag{5}$$

where a_t is the theoretically predicted constant of proportionality (Thamdrup et al. 2007). From the above equation, it can be noted that L^2 is directionally proportional to t.

For microchannel with $w >> h$, we can consider Poiseuille flow for infinite parallel-plate condition.

$$Q = \frac{d^3 \times w \times P_c}{12\eta L} \tag{6}$$

Where Q is the flow rate and P_c is capillary pressure.

The velocity field for the Poiseuille flow in a rectangular microchannel is given by Eq. 7 (Bruus 2008).

$$u(y,z) = \frac{4d^2 \times \sigma_{PCR}}{\pi^3 \times \eta_{PCR} \times L} \times \left(\frac{cos\theta_g + cos\theta_p}{d} + \frac{2cos\theta_p}{w}\right) \sum_{i,odd}^{\bowtie} \frac{1}{i^3}\left[1 - \frac{cosh\left(i\pi\frac{y}{d}\right)}{cosh\left(i\pi\frac{w}{2d}\right)}\right] sin\left(i\pi\frac{z}{d}\right) \tag{7}$$

Computation fluid dynamics (CFD) software was used to understand the cross-section of the meniscus shape in PDMS-glass hybrid channels, and movement of capillary meniscus with respect to time. In order to evaluate the cross-section of the meniscus, Eq. 7 was plotted using Matlab software (Version R2011a). The velocity profile is shown in Fig. 7a. This figure depicts the marching velocity of the capillary meniscus in a microchannel. The exact velocity variation along the x-direction is of minor concern in this model. However, the change in contact angle can significantly affect the profile.

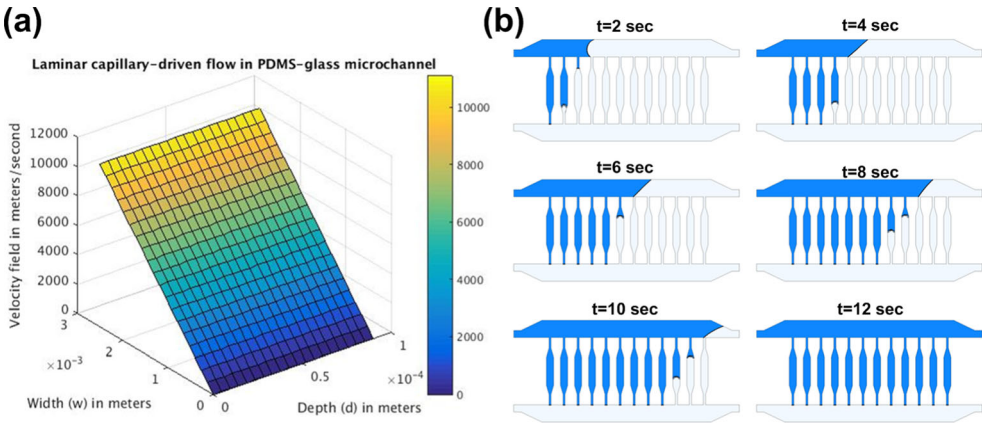

Fig. 7 **a** Capillary meniscus in a microchannel with hydrophobic (PDMS) and hydrophilic (glass) walls, and **b** the transient filling of microchannel at six different time point obtained using CFD model

Similar capillary meniscus profile and behaviour was reported by Kim et al. (Kim et al. 2010).

In order to simulate meniscus movement inside the PDMS-glass hybrid microchannel, we used ANSYS Fluent software and experimentally validated the simulated data. In literature, many groups have studied capillary meniscus movement in microchannels (Chan and Yang 2005, Lung-Jieh et al. 2004; Waghmare and Mitra 2012). Yang et al. measured the marching velocity of capillary menisci in microchannels (Lung-Jieh et al. 2004). The authors reported an analytical model to calculate the marching velocity of the meniscus. In this model, the velocity profile was assumed parabolic and the pressure difference across the liquid-gas interface was calculated using the "Laplace pressure drop". Neglecting the acceleration term, they found that the position of the interfaces was proportional to the square root of time. Yang et al. reported theoretical modelling of two-immiscible water-silicone oil displacement in a circular capillary. In this model, a dynamic contact angle approach was implemented, and the experimental data was found to be in-agreement with the theoretical predictions (Chan and Yang 2005). Recently, Mitra and colleagues presented a comprehensive theoretical model for capillary flow analyses using transient velocity profile instead of the widely used fully developed velocity profile (Waghmare and Mitra 2012).

3.4.3 CFD modelling

The ANSYS Fluent 14.5 (Fluent Inc., Lebanon, NH) software has been used to solve the flow of the PCR filling the microchannel. A second order upwind scheme is applied for the spatial momentum discretization, and pressure staggering option (PRESTO) scheme was used for pressure discretization. The pressure implicit solution by split order (PISO) algorithm is employed to couple the pressure with the velocity in the incompressible limit. The Volume of Fluid (VOF) model has enabled the capturing and tracking of the multiphase interface where the scalar advection equation for the indicator function is solved with the Navier-Stokes equations. The appropriate evaluation of the fluxes across the element faces of the advection terms has been achieved by the geometric reconstruction based on the PLIC scheme. The simulated images of flow front in PDMS-glass hybrid chip is shown in Fig. 7b and also supplementary movie 1.

In order to experimentally determine the position of meniscus inside the PDMS-glass micro-channel with respect to time, a microchip device with dimensions mentioned in Table 1 was fabricated. The PCR solution was loaded at the mouth the inlet channel and the movement of capillary meniscus in the PDMS-glass hybrid inlet channel with respect to time is monitored using a SONY camcorder (Model: DCR-HC 38, 40× optical zoom capability with Carl Zeiss® Vario-Tessar® Lens). A scale with 1 mm pitch was included to measure of capillary displacement. The image sequence

Table 1 Inlet channel dimension and value of other parameters used in simulation (values at 293 K)

Parameters	Symbols	Values
Length of the inlet channel	L_{in}	24 mm
Width of the inlet channel	w	2.5 mm
Depth of the inlet channel	d	~0.09 mm
Operation temperature	T_{ref}	293 K
Atmospheric/reference pressure	P_{ref}	1e5 Pa
Density of air	ρ_{air}	1.225 $\frac{Kg}{m^3}$
Dynamic viscosity of air	η_{air}	1.789 e-5 $Pa \cdot$ sec
Density of PCR solution	ρ_{PCR}	1000 $\frac{Kg}{m^3}$
Dynamic viscosity of PCR solution	η_{PCR}	1e-3 $Pa \cdot$ sec
Kinematic viscosity of PCR solution	ν_{PCR}	1e-6 $\frac{m^2}{s}$
Surface tension of PCR solution	σ_{PCR}	30.8e-3 $\frac{N}{m}$
Contact angle of PCR solution on PDMS	θ_p	46° (0.8 rad)
Contact angle of PCR solution on glass	θ_g	14° (0.24 rad)

extracted from this video is shown in Fig. 8. The experimental and numerical data for the L^2 as a function of time is shown in Fig. 9. It can be seen that there is a good agreement between numerical and experimental results.

4 Conclusions

In this paper, we report simulation and experimental validation of capillary-driven flow in PDMS-glass hybrid ladder network. The fluid parameters such as surface-tension and contact angle (on materials used in devices reported in this study) of the PCR solution is extensively characterized in the context of capillary-driven flow. The estimated fluid parameters were used for numerical simulation of capillary meniscus movement in PDMS-glass hybrid microchannel. Numerical modelling using PRESTO scheme was used to study the movement of capillary filling front in a complex PDMS-glass hybrid microchannel. The results from numerical model prediction was compared with the experimental results

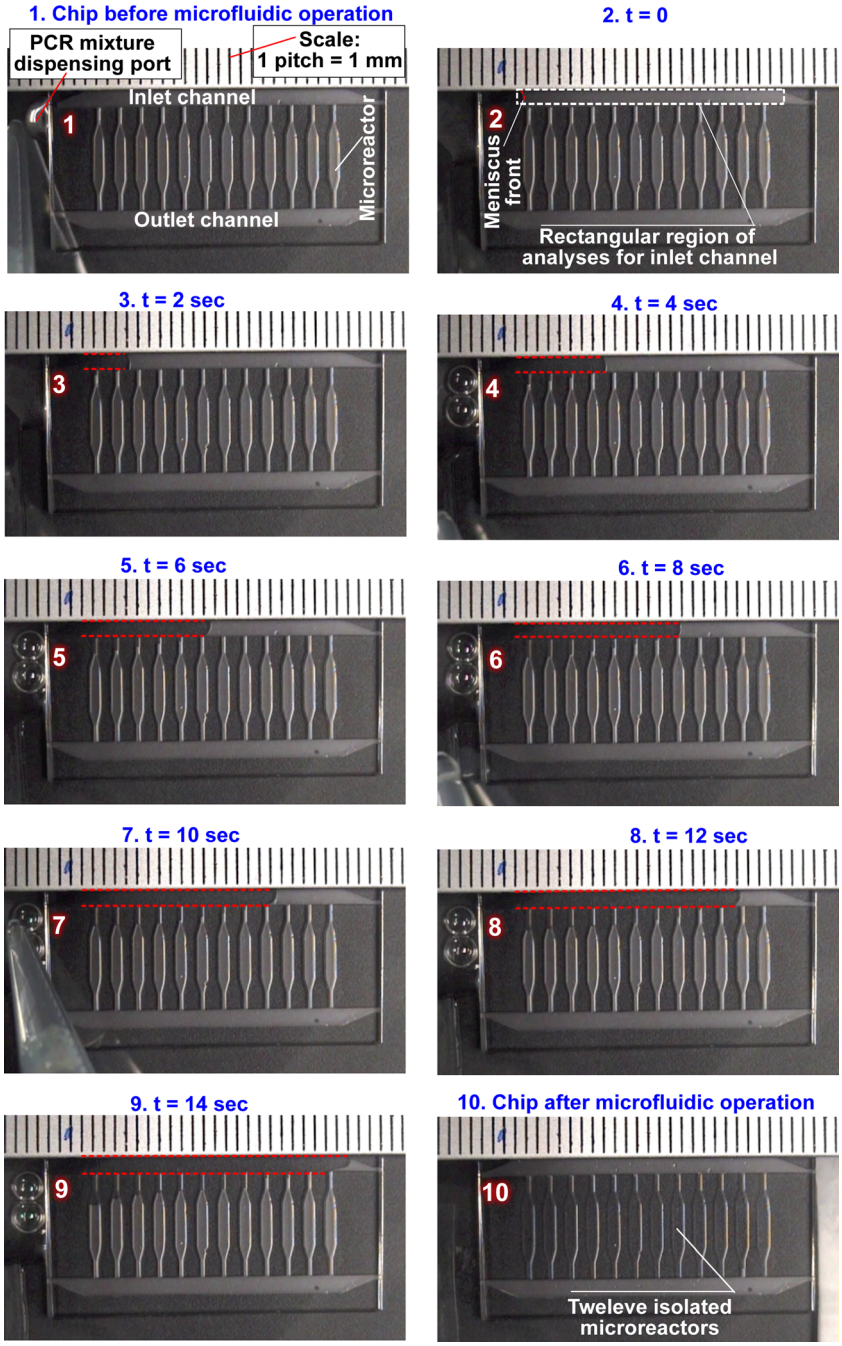

Fig. 8 Displacement of capillary meniscus as a function of time inside a microfluidic biochip with 12 reaction chambers

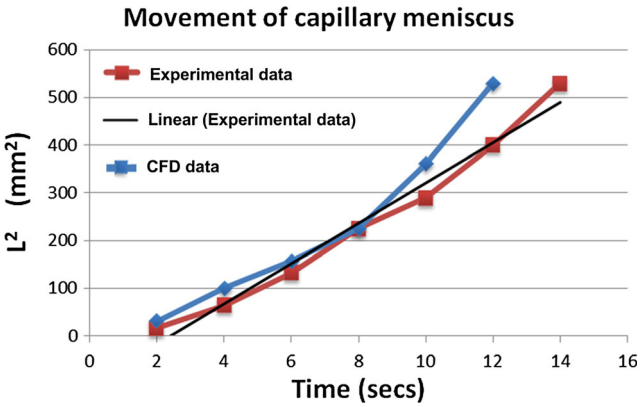

Fig. 9 Displacement of capillary meniscus as a function of time obtained using experimental and numerical results

and found to be comparable. Based on visual comparison, the shape of meniscus was found to match between the numerical model and experiment data.

References

A. K. Au, H. Lai, B. R. Utela, A. Folch, Microvalves and micropumps for BioMEMS. Micromachines **2**, 179–220 (2011). doi:10.3390/mi2020179

B. Bachmann, W. Luke, G. Hunsmann, Improvement of PCR amplified DNA sequencing with the aid of detergents. Nucleic Acids Res. **18**, 1309 (1990)

H. Bruus, *Theoretical microfluidics*. (OUP, Oxford, 2008), p. 51

W. K. Chan, C. Yang, Surface-tension-driven liquid–liquid displacement in a capillary. J. Micromech. Microeng. **15**, 1722 (2005)

P.-C. Chen, W. Fan, T.-K. Hoo, L. C. Z. Chan, Z. Wang, Simulation guided-design of a microfluidic thermal reactor for polymerase chain reaction. Chem. Eng. Res. Des. **90**, 591–599 (2012). doi:10.1016/j.cherd.2011.09.00

E. Delamarche, A. Bernard, H. Schmid, B. Michel, H. Biebuyck, *Patterned delivery of immunoglobulins to surfaces using microfluidic networks*, vol 276 (Science, 1997), pp. 779–781

L. Gervais, E. Delamarche, Toward one-step point-of-care immunodiagnostics using capillary-driven microfluidics and PDMS substrates. Lab Chip **9**, 3330–3337 (2009). doi:10.1039/b906523g

L. Gui, C. L. Ren, Numeric simulation of heat transfer and electrokinetic flow in an electroosmosis-based continuous flow PCR chip. Anal. Chem. **78**, 6215–6222 (2006). doi:10.1021/ac060553d

K. Hosokawa, M. Omata, K. Sato, M. Maeda, Power-free sequential injection for microchip immunoassay toward point-of-care testing. Lab Chip **6**, 236–241 (2006). doi:10.1039/b513424b

J. Hu, S. Wang, L. Wang, F. Li, B. Pingguan-Murphy, T. J. Lu, F. Xu, Advances in paper-based point-of-care diagnostics. Biosens. Bioelectron. **54**, 585–597 (2014). doi:10.1016/j.bios.2013.10.075

H. E. Jeong, P. Kim, M. K. Kwak, C. H. Seo, K. Y. Suh, Capillary kinetics of water in homogeneous, hydrophilic polymeric micro- to nanochannels. Small **3**, 778–782 (2007). doi:10.1002/smll.200600666

D. Juncker, H. Schmid, U. Drechsler, H. Wolf, M. Wolf, B. Michel, N. de Rooij, E. Delamarche, Autonomous microfluidic capillary system. Anal. Chem. **74**, 6139–6144 (2002)

A. Karagunduz, K. D. Pennell, M. H. Young, Influence of a nonionic surfactant on the water retention properties of unsaturated soils. Soil Sci. Soc. Am. J. **65**, 1392–1399 (2001). doi:10.2136/sssaj2001.6551392x

E. Kim, Y. Xia, G. M. Whitesides, Polymer microstructures formed by moulding in capillaries. Nature **376**, 581–584 (1995)

Y. C. Kim, S.-H. Kim, D. Kim, S.-J. Park, J.-K. Park, Plasma extraction in a capillary-driven microfluidic device using surfactant-added poly(-dimethylsiloxane). Sensors Actuators B Chem. **145**, 861–868 (2010). doi:10.1016/j.snb.2010.01.017

Y. Lung-Jieh, Y. Tze-Jung, T. Yu-Chong, The marching velocity of the capillary meniscus in a microchannel. J. Micromech. Microeng. **14**, 220 (2004)

N. Ramalingam, H.-B. Liu, C.-C. Dai, Y. Jiang, H. Wang, Q. Wang, K. M. Hui, H.-Q. Gong, Real-time PCR array chip with capillary-driven sample loading and reactor sealing for point-of-care applications. Biomed. Microdevices **11**, 1007–1020 (2009)

N. Ramalingam, Z. Rui, H.-B. Liu, C.-C. Dai, R. Kaushik, B. Ratnaharika, H.-Q. Gong, Real-time PCR-based microfluidic array chip for simultaneous detection of multiple waterborne pathogens. Sensors Actuators B Chem. **145**, 543–552 (2010). doi:10.1016/j.snb.2009.11.025

G. C. Randall, P. S. Doyle, Permeation-driven flow in poly(dimethylsiloxane) microfluidic devices. Proc. Natl. Acad. Sci. U. S. A. **102**, 10813–10818 (2005). doi:10.1073/pnas.0503287102

R. Safavieh, D. Juncker, Capillarics: pre-programmed, self-powered microfluidic circuits built from capillary elements. Lab Chip **13**, 4180–4189 (2013). doi:10.1039/c3lc50691f

R. Safavieh, A. Tamayol, D. Juncker, Serpentine and leading-edge capillary pumps for microfluidic capillary systems. Microfluid. Nanofluid., 1–10 (2014). doi:10.1007/s10404-014-1454-3

T. M. Schutzius, M. Elsharkawy, M. K. Tiwari, C. M. Megaridis, Surface tension confined (STC) tracks for capillary-driven transport of low surface tension liquids. Lab Chip **12**, 5237–5242 (2012). doi:10.1039/c2lc40849j

J. Seo, L. P. Lee, Effects on wettability by surfactant accumulation/depletion in bulk polydimethylsiloxane (PDMS). Sensors Actuators B Chem. **119**, 192–198 (2006)

J. Siegrist, M. Amasia, N. Singh, D. Banerjee, M. Madou, Numerical modeling and experimental validation of uniform microchamber filling in centrifugal microfluidics. Lab Chip **10**, 876–886 (2010). doi:10.1039/b917880e

H. Tachibana, M. Saito, K. Tsuji, K. Yamanaka, L. Q. Hoa, E. Tamiya, Self-propelled continuous-flow PCR in capillary-driven microfluidic device: microfluidic behavior and DNA amplification. Sensors Actuators B Chem. **206**, 303–310 (2015). doi:10.1016/j.snb.2014.09.004

L. H. Thamdrup, F. Persson, H. Bruus, A. Kristensen, H. Flyvbjerg, Experimental investigation of bubble formation during capillary filling of SiO[sub 2] nanoslits. Appl. Phys. Lett. **91**, 163505–163503 (2007)

P. Waghmare, S. Mitra, A comprehensive theoretical model of capillary transport in rectangular microchannels. Microfluid. Nanofluid. **12**, 53–63 (2012). doi:10.1007/s10404-011-0848-8

G. M. Walker, D. J. Beebe, A passive pumping method for microfluidic devices. Lab Chip **2**, 131–134 (2002). doi:10.1039/b204381e

S. Wang, W. Wang, Kinetic characteristics of continuous flow polymerase chain reaction chip: A numerical investigation. SCIENCE CHINA Technol. Sci. **53**, 1967–1972 (2010). doi:10.1007/s11431-010-3096-3

R. S. Weyant, P. Edmonds, B. Swaminathan, Effect of ionic and nonionic detergents on the Taq polymerase. Biotechniques **9**, 308–309 (1990)

K. S. Yun, E. Yoon, Micro/Nanofluidic device for single-cell-based assay. Biomed. Microdevices **7**, 35–40 (2005)

C. Zhang, D. Xing, Miniaturized PCR chips for nucleic acid amplification and analysis: latest advances and future trends. Nucleic Acids Res. **35**, 4223–4237 (2007). doi:10.1093/nar/gkm389

M. Zimmermann, H. Schmid, P. Hunziker, E. Delamarche, Capillary pumps for autonomous capillary systems. Lab Chip **7**, 119–125 (2007). doi:10.1039/b609813d